Numerical study of heat transfer from an offshore buried pipeline under steady–periodic thermal boundary conditions

A. Barletta, E. Zanchini, S. Lazzari, A. Terenzi

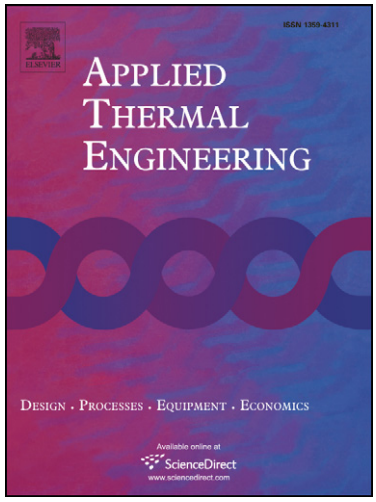

Numerical study of heat transfer from an offshore buried pipeline under steady–periodic thermal boundary conditions

A. Barletta, E. Zanchini, S. Lazzari, A. Terenzi

PII: S1359-4311(07)00281-5
DOI: 10.1016/j.applthermaleng.2007.08.004
Reference: ATE 2246

To appear in: *Applied Thermal Engineering*

Received Date: 15 November 2006
Revised Date: 1 August 2007
Accepted Date: 14 August 2007

Please cite this article as: A. Barletta, E. Zanchini, S. Lazzari, A. Terenzi, Numerical study of heat transfer from an offshore buried pipeline under steady–periodic thermal boundary conditions, *Applied Thermal Engineering* (2007), doi: 10.1016/j.applthermaleng.2007.08.004

Numerical study of heat transfer from an offshore buried pipeline under steady–periodic thermal boundary conditions

A. Barletta *♮ - E. Zanchini * - S. Lazzari * - A. Terenzi °

* Università di Bologna. Dipartimento di Ingegneria Energetica, Nucleare e del Controllo Ambientale (DIENCA). Laboratorio di Montecuccolino. Via dei Colli, 16. I–40136 Bologna, Italy.

antonio.barletta@unibo.it ; enzo.zanchini@unibo.it ; stefano.lazzari@unibo.it

♮ Corresponding Author: Prof. Antonio Barletta, Tel. ++39 051 6441703, Fax. ++39 051 6441747.

° Snamprogetti S.p.A. Via Toniolo, 1. I-61032. Fano (PS), Italy.

alessandro.terenzi@snamprogetti.eni.it

Abstract

The steady–periodic heat transfer between offshore buried pipelines for the transport of hydrocarbons and their environment is investigated. This heat transfer regime occurs for shallow water buried pipelines, as a consequence of the temperature changes of the seabed during the year. First, the unsteady two dimensional conduction problem is written in a dimensionless form; then, it is transformed into a steady two dimensional problem and solved numerically by means of the finite–element software package Comsol Multiphysics (© Comsol, Inc.). Several values of the burying depth and of the radius of the pipeline, as well as of the thermal properties of the soil are considered. The numerical results are compared with those obtainable by means of an approximate method employed in industrial design. The comparison reveals that important discrepancies with respect to this approximate method may occur.

Keywords — Offshore buried pipelines; Heat transfer; Steady–periodic boundary conditions; Numerical methods; Industrial design

List of symbols

A, B	dimensionless coefficients
a	dimensionless length
C	dimensionless constant defined in Eq.(A2)
c_v	soil specific heat at constant volume
H	burying depth of the pipeline
k	soil conductivity
$\vec{n}$	normal unit vector
q	thermal power per unit area
$\dot{Q}$	thermal power per unit length
$\dot{Q}_{const}$	thermal power per unit length, in the constant power limit
$\dot{Q}_{qs}$	thermal power per unit length, in the quasi–stationary limit
R	pipeline radius
T_a	pipeline wall temperature
T_e	seabed temperature
T_{eff}	effective temperature
T_H	soil temperature at a depth H
T_m	mean annual seabed temperature
T_0, T_1, T_2	temperature fields
t	time
X, Y	coordinates
x, y	dimensionless coordinates

Greek Symbols

α	soil thermal diffusivity
β, γ	dimensionless quantities defined in Eq.(A4)
ΔT	amplitude of temperature oscillations
$\theta_0, \theta_1, \theta_2$	dimensionless temperature fields

Λ_0	dimensionless heat transfer coefficient
Ξ	dimensionless parameter
ρ	soil density
σ	dimensionless burying depth
Σ	dimensionless parameter
ϕ	phase angle defined in Eq.(A3)
ω	angular frequency

Superscripts, subscripts

$*$	dimensionless quantity
max	maximum value
min	minimum value

1 Introduction

As is well known, offshore buried pipelines are often used for the transport of hydrocarbons from extraction sites to refinement plants. The design of these pipelines requires the knowledge of the overall heat transfer coefficient from the pipe wall to the environment. In fact, a significant decrease of the fluid temperature could cause the formation of hydrates and waxes which might stop the fluid flow. Moreover, the knowledge of the bulk temperature of the fluid in any cross section is necessary to determine the value of the fluid viscosity in that section and, thus, to evaluate the viscous pressure drop along the flow direction. As a consequence, the heat transfer from buried pipelines has been widely studied in the literature [1]–[4]. An analytical expression of the steady–state heat transfer coefficient from an offshore buried pipeline to its environment can be found in [5]. It refers to the boundary condition of a uniform temperature of the seabed, *i.e.* of the separation surface between soil and sea water. In these conditions, the thermal power exchanged between the pipeline and its environment, per unit length of the duct, can be

expressed as

$$\dot{Q} = k\,(T_a - T_e)\,\Lambda_0 \quad , \tag{1}$$

where k is the thermal conductivity of the soil, T_a is the temperature of the external surface of the duct, T_e is the temperature of the seabed and Λ_0 is a dimensionless heat transfer coefficient, given by

$$\Lambda_0\,(\sigma) = \frac{2\pi}{\operatorname{arccosh}\,(\sigma)} \quad . \tag{2}$$

In Eq. (2), σ is the ratio between the burying depth of the pipe axis, H, and the external radius of the pipe, R.

Equations (1) and (2) provide reliable results in many cases, but cannot be applied, for instance, in the following circumstance. For shallow–water pipelines, the temperature of the seabed is affected by the season changes and varies accordingly during the year. With reference to the Mediterranean sea, the seabed statistically reaches a minimum value of 14°C, in winter, and a maximum value of 25°C, in summer. Clearly, this temperature change of the seabed may have a strong influence on the thermal power exchanged between the pipeline and its environment.

At present, an approximate method is employed in industrial design to take into account this effect. The soil is considered as a semi–infinite solid medium whose surface temperature varies in time according to the law

$$T = T_m + \Delta T \sin\,(\omega\,t) \quad , \tag{3}$$

where T_m is the mean annual temperature of the seabed, ΔT is the amplitude of the temperature oscillation and ω is the angular frequency which corresponds to the period of one year, namely

$$\omega = 0.1991 \cdot 10^{-6}\ \mathrm{s}^{-1} \quad . \tag{4}$$

Thus, by assuming that the pipeline does not modify considerably the temperature distribution in the soil, at a depth H one has [6]

$$T_H = T_m - \Delta T\,\exp\left(-\sqrt{\frac{\omega}{2\alpha}}\,H\right)\,\sin\left(\sqrt{\frac{\omega}{2\alpha}}\,H - \omega\,t\right) \quad , \tag{5}$$

where α is the thermal diffusivity of the soil. In the approximate method, the thermal power is evaluated as

$$\dot{Q} = k\,(T_a - T_H)\,\Lambda_0 \quad , \tag{6}$$

i.e. by replacing T_e with T_H in Eq. (1).

The approximate method does not seem reliable because it is not based on a rigorous mathematical model. To check the reliability of the method, one can apply it to evaluate the heat transfer between a plane isothermal surface buried at a depth H and the surrounding soil, when the temperature of the ground surface varies in time according to Eq.(3). In fact, for this case, an analytical expression of the soil temperature field is available in the literature [7]. This analysis has been performed with reference to standard properties of the soil and is reported in Appendix. The comparison between the analytical solution and the approximate method shows that the latter yields acceptable results only when very small values of H are considered. Therefore, a more reliable method to evaluate the steady–periodic heat transfer from buried pipelines to the environment is needed.

The aim of this investigation is to find out an accurate method to determine the heat transfer between an offshore buried pipeline and its environment in steady–periodic conditions. First, by introducing suitable auxiliary variables, the unsteady two dimensional conduction problem is transformed into a steady two dimensional problem in the new variables. Then, the steady problem is solved numerically by means of the software package COMSOL Multiphysics (© Comsol, Inc.). The results show that the empirical method given by Eqs. (6), (5) and (2) may yield a too rough approximation in some cases.

2 Mathematical model

Let us assume that the temperature of the seabed varies in time according to Eqs. (3) and (4). The computational domain and the boundary conditions are sketched in Figure 1. As is shown in the figure, the vertical and bottom boundaries of the computational domain

are considered as adiabatic. The differential equation to be solved is Fourier equation

$$\frac{\partial T}{\partial t} = \alpha \, \nabla^2 T \quad , \tag{7}$$

with the following boundary conditions:

$$T = T_a \quad \text{on the pipe surface;} \tag{8}$$

$$T = T_m + \Delta T \sin(\omega t) \quad \text{on the seabed;} \tag{9}$$

$$\vec{n} \cdot \vec{\nabla} T = 0 \quad \text{on the vertical and bottom boundaries.} \tag{10}$$

In steady–periodic regime, the temperature field can be expressed as

$$\begin{aligned} T(X,Y,t) &= T_0(X,Y) \\ &\quad + [T_1(X,Y) - T_m] \, \sin(\omega t) + [T_2(X,Y) - T_m] \, \cos(\omega t) \quad . \end{aligned} \tag{11}$$

By substituting Eq. (11) in Eq. (7), one obtains

$$\begin{aligned} &\omega (T_1 - T_m) \cos(\omega t) - \omega (T_2 - T_m) \sin(\omega t) = \\ &\alpha \left[\nabla^2 T_0 + \nabla^2 T_1 \sin(\omega t) + \nabla^2 T_2 \cos(\omega t) \right] \quad . \end{aligned} \tag{12}$$

Equation (12) implies

$$\nabla^2 T_0 = 0 \quad , \tag{13}$$

$$\alpha \, \nabla^2 T_1 = -\omega (T_2 - T_m) \quad , \tag{14}$$

$$\alpha \, \nabla^2 T_2 = \omega (T_1 - T_m) \quad . \tag{15}$$

The boundary conditions for T_0, T_1 and T_2 are:

$$T_0 = T_a \quad , \quad T_1 = T_2 = T_m \quad \text{on the pipe surface;} \tag{16}$$

$$T_0 = T_m \quad , \quad T_1 = T_m + \Delta T \quad , \quad T_2 = T_m \quad \text{on the seabed;} \tag{17}$$

$$\vec{n} \cdot \vec{\nabla} T_0 = 0 \quad , \quad \vec{n} \cdot \vec{\nabla} T_1 = 0 \quad , \quad \vec{n} \cdot \vec{\nabla} T_2 = 0$$

$$\text{on the vertical and bottom boundaries.} \tag{18}$$

The thermal power exchanged between the pipeline and the environment can be evaluated by means of the expression

$$\dot{Q} = k \left[\int_{\partial L} \vec{n} \cdot \vec{\nabla} T_0 \; dl \; + \; \left(\int_{\partial L} \vec{n} \cdot \vec{\nabla} T_1 \; dl \right) \; \sin(\omega\, t) \right.$$
$$\left. + \; \left(\int_{\partial L} \vec{n} \cdot \vec{\nabla} T_2 \; dl \right) \cos(\omega\, t) \right] \quad , \tag{19}$$

where ∂L is the circular boundary of the duct, dl is the infinitesimal arc of this boundary and $\vec{n}$ is the unit vector orthogonal to ∂L, as illustrated in Figure 1.

Let us introduce the following dimensionless variables:

$$\theta_0 = \frac{T_0 - T_m}{\Delta T} \;\; , \;\; \theta_1 = \frac{T_1 - T_m}{\Delta T} \;\; , \;\; \theta_2 = \frac{T_2 - T_m}{\Delta T} \;\; ,$$
$$x = \frac{X}{R} \;\; , \;\; y = \frac{Y}{R} \;\; , \;\; \vec{\nabla}^* = R\, \vec{\nabla} \;\; ,$$
$$\Omega = \frac{\omega\, R^2}{\alpha} \;\; , \;\; \Xi = \frac{\Delta T}{T_a - T_m} \;\; . \tag{20}$$

Equations (13)–(18) can be written in the dimensionless form

$$\nabla^{*2} \theta_0 = 0 \;\; ; \tag{21}$$

$$\nabla^{*2} \theta_1 = -\, \Omega \; \theta_2 \;\; ; \tag{22}$$

$$\nabla^{*2} \theta_2 = \;\; \Omega \; \theta_1 \;\; ; \tag{23}$$

$$\theta_0 = \frac{1}{\Xi} \;\; , \;\; \theta_1 = 0 \;\; , \;\; \theta_2 = 0 \quad \text{on the pipe surface;} \tag{24}$$

$$\theta_0 = 0 \;\; , \;\; \theta_1 = \;\; 1 \;\; , \;\; \theta_2 = 0 \quad \text{on the seabed;} \tag{25}$$

$$\vec{n} \cdot \vec{\nabla}^* \theta_0 = 0 \;\; , \;\; \vec{n} \cdot \vec{\nabla}^* \theta_1 = 0 \;\; , \;\; \vec{n} \cdot \vec{\nabla}^* \theta_2 = 0 \quad \text{on vertical and bottom sides.} \tag{26}$$

By means of Eq. (20), one can write Eq. (19) in the form

$$\dot{Q} = k\, (T_a - T_m)\; \Xi \left[\int_{\partial L^*} \vec{n} \cdot \vec{\nabla}^* \theta_0 \; dl^* \right.$$

$$+ \left(\int\limits_{\partial L^*} \vec{n} \cdot \vec{\nabla}^* \theta_1 \; dl^* \right) \sin(\omega\, t) + \left(\int\limits_{\partial L^*} \vec{n} \cdot \vec{\nabla}^* \theta_2 \; dl^* \right) \cos(\omega\, t) \Bigg] \quad . \tag{27}$$

The boundary value problem for the dimensionless temperature field θ_0 is the steady conduction problem already solved in [5]. Therefore, the first integral in Eq. (27) is such that

$$\Xi \int\limits_{\partial L^*} \vec{n} \cdot \vec{\nabla}^* \theta_0 \; dl^* = \Lambda_0(\sigma) = \frac{2\pi}{\operatorname{arccosh}(\sigma)} \quad . \tag{28}$$

In order to determine the dimensionless fields θ_1 and θ_2, one can solve numerically the coupled differential equations (22) and (23), with the boundary conditions prescribed in Eqs. (24)–(26). The solution depends on the dimensionless parameters σ and Ω.

By employing the dimensionless heat transfer coefficient Λ_0 and the dimensionless quantities

$$A = \frac{1}{\Lambda_0} \int\limits_{\partial L^*} \vec{n} \cdot \vec{\nabla}^* \theta_1 \; dl^* \quad , \quad B = \frac{1}{\Lambda_0} \int\limits_{\partial L^*} \vec{n} \cdot \vec{\nabla}^* \theta_2 \; dl^* \quad , \tag{29}$$

one can rewrite Eq. (27) in the form

$$\dot{Q} = k\,(T_a - T_m)\; \Lambda_0 \; \{1 \; + \; \Xi \; [A \; \sin(\omega\, t) + \; B \; \cos(\omega\, t)]\} \quad . \tag{30}$$

Since Λ_0 is known, Eq. (30) allows one to evaluate the time–dependent thermal power exchanged between the pipeline and its environment by employing tables of A and B, which are functions of the dimensionless parameters σ and Ω.

2.1 Values of the dimensionless parameters

In technical applications, the depth H of the pipeline axis can range from the duct radius R to about ten times R. Indeed, the following values of σ have been considered: 1.2; 1.5; 2.0; 4.0; 10.0 .

The period of the temperature oscillation is one year; thus, ω is given by Eq. (4). The thermal properties of the soil vary in the ranges:

$$k_{\min} = 1 \;\; \frac{\mathrm{W}}{\mathrm{m\,K}} \quad , \quad k_{\max} = 3 \;\; \frac{\mathrm{W}}{\mathrm{m\,K}} \quad , \tag{31}$$

$$\rho_{\min} = 1.2 \cdot 10^3 \;\; \frac{\mathrm{kg}}{\mathrm{m}^3} \quad , \quad \rho_{\max} = 2.5 \cdot 10^3 \;\; \frac{\mathrm{kg}}{\mathrm{m}^3} \quad , \tag{32}$$

$$c_{v\,\min} = 1 \cdot 10^3 \ \frac{\mathrm{J}}{\mathrm{kg\,K}} \ , \ \ c_{v\,\max} = 2 \cdot 10^3 \ \frac{\mathrm{J}}{\mathrm{kg\,K}} \ . \tag{33}$$

Therefore, one has

$$\alpha_{\min} = \frac{k_{\min}}{\rho_{\max}\ c_{v\,\max}} = 2.0 \cdot 10^{-7} \ \frac{\mathrm{m}^2}{\mathrm{s}} \ , \quad \alpha_{\max} = \frac{k_{\max}}{\rho_{\min}\ c_{v\,\min}} = 2.5 \cdot 10^{-6} \ \frac{\mathrm{m}^2}{\mathrm{s}} \ . \tag{34}$$

In offshore buried pipelines for the transport of hydrocarbons, the duct diameter varies from six to forty inches, *i.e.* the radius varies in the range

$$R_{\min} = 7.6 \ \ \mathrm{cm} \ , \ \ R_{\max} = 0.51 \ \ \mathrm{m} \ . \tag{35}$$

From these data, one obtains

$$\Omega_{\min} = \frac{\omega\, R_{\min}^2}{\alpha_{\max}} = 4.6 \cdot 10^{-4} \ , \ \ \Omega_{\max} = \frac{\omega\, R_{\max}^2}{\alpha_{\min}} = 0.26 \ . \tag{36}$$

The following values of Ω have been considered: 0.0003; 0.001; 0.01; 0.05; 0.1; 0.3 .
As for the dimensionless parameter Ξ, which does not appear in numerical computations, let us point out that its minimum absolute value occurs when $T_a - T_m$ is maximum. Since in practical cases $T_{a\,\max} \approx 50$ °C, with reference to the Mediterranean sea, where $T_m = 19.5$ °C and $\Delta T = 5.5$ °C, one has

$$|\Xi|_{\min} = \frac{5.5}{30.5} = 0.18 \ . \tag{37}$$

Clearly, Eq. (30) allows one to evaluate the thermal power $\dot{Q}$ for every value of Ξ.

3 Results

The dimensionless boundary value problem for the unknown functions θ_1 and θ_2, given by Eqs. (22)–(26), has been solved numerically by means of the finite–element computational code COMSOL Multiphysics (© Comsol, Inc.). Since the dimensionless computational domain and the boundary conditions are symmetric with respect to the plane $x = 0$, only half domain has been considered in the computations and the adiabatic condition on the symmetry axis has been imposed, as sketched in Figure 2. The final computations have been performed with $a = 100$, where a is both the dimensionless depth (starting from the

pipeline axis) and the dimensionless width of the actual computational domain, as shown in Figure 2. Indeed, preliminary calculations revealed that this value of a is sufficiently high to ensure accurate results.

Unstructured grids with triangular elements have been used. The grids have been refined close to the boundaries 1, 6 and 5, and in a square region around the duct (see Figure 3). After some checks to ensure the grid–independence, the final computations have been performed with about $5 \cdot 10^4$ grid elements.

The values of the coefficients A and B given by Eq. (29) are determined by COMSOL Multiphysics as follows. The x–component and the y–component of the gradient of θ_1 and θ_2 are multiplied by the x–component and y–component of the unit vector normal to the boundary surface **5** (see Figure 2). The latter components are built–in variables denoted as `nx` and `ny`. Then, A and B are evaluated in postprocessing through the `Boundary Integration` option.

The results obtained for the coefficients A and B are reported in Table 1 for $\sigma = 1.2$ and $\sigma = 1.5$, in Table 2 for $\sigma = 2$ and $\sigma = 4$, in Table 3 for $\sigma = 6$ and $\sigma = 10$.

In order to illustrate the effects of the temperature oscillations at the seabed on the heat transfer rate between the pipe and its environment, let us compare the thermal power exchanged in steady–periodic regime, given by Eq. (30), with two limiting cases. In the limit of very high values of H and very low values of α, *i.e.* for very high values of both σ and Ω, the effect of the temperature oscillations at the seabed on the heat transfer rate becomes negligible. In this limit, which will be called *constant power limit*, the sea temperature oscillations affect only a thin soil layer close to the seabed, far from the pipe, so that the thermal power exchanged between the pipeline and its environment is constant and is given by

$$\dot{Q}_{const} = k\,(T_a - T_m)\,\Lambda_0 \quad . \tag{38}$$

On the other hand, in the limit of σ very close to 1 and of very low values of Ω, one can assume that the temperature oscillations have a uniform phase. In this limit, which will be called *quasi–stationary limit*, the thermal power exchanged between pipeline and environment can be evaluated, at any time instant, by considering steady–state conditions

with a temperature at the seabed given by the temperature at that instant. Thus, in the *quasi–stationary limit*, one has

$$\dot{Q}_{qs} = k\,(T_a - T_m)\;\Lambda_0\;[1 - \Xi\;\sin(\omega\,t)] \quad . \tag{39}$$

A comparison between Eqs. (30) and (38) reveals that the general expression for the steady–periodic thermal power coincides with $\dot{Q}_{const}$ (*constant power limit*) when $A = B = 0$. A comparison between Eqs. (30) and (39) reveals that the general expression for the steady–periodic thermal power coincides with $\dot{Q}_{qs}$ (*quasi-stationary limit*) when $A = -1$ and $B = 0$. Indeed, the results reported in Table 3 point out that, for $\sigma = 10$ and $\Omega = 0.3$, the values of A and B are very close to zero, *i.e.* the *constant power limit* is approached. On the other hand, the results reported in Table 1 point out that, for $\sigma = 1.2$ and $\Omega = 0.0003$, $A \approx -1$ and $B \approx 0$, so that the quasi–stationary limit is nearly reached.

The amplitude of the dimensionless temperature oscillations $\sqrt{\theta_1^2 + \theta_2^2}$ is illustrated in Figure 4 for $\sigma = 10$ and $\Omega = 0.3$. The figure shows that the temperature oscillations are negligible at the depth of the pipe, so that a nearly constant heat flux from the duct wall occurs (*constant power limit*).

The amplitude $\sqrt{\theta_1^2 + \theta_2^2}$ and the phase $\arctan(\theta_2\,/\theta_1)$ of the dimensionless temperature oscillations, for $\sigma = 1.2$ and $\Omega = 0.0003$, are illustrated in Figures 5 and 6 respectively. Figure 5 shows that important temperature oscillations take place in the soil even at depths greater than that of the pipe, except very close to the pipe boundary, where a constant temperature boundary condition has been imposed.

Figure 6 shows that the phase is nearly uniform and next to zero even at depths higher than that of the pipe. Thus, the *quasi–stationary limit* can be applied with an excellent approximation in this case. In most cases, neither the *constant power limit* not the *quasi–stationary limit* can be applied, and the power exchanged between the pipe and its environment must be calculated by means of Eq. (30) and of Tables 1, 2 and 3.

In order to compare the results presented in this paper with the approximate results

obtainable by means of Eq. (6), let us rewrite Eq. (30) in the form

$$\dot{Q} = k\,(T_a - T_{eff})\;\Lambda_0 \quad , \tag{40}$$

where the effective temperature T_{eff} is given by

$$T_{eff} = T_m - \Delta T\;\left[A\;\sin(\omega\,t) + B\;\cos(\omega\,t)\right] \quad . \tag{41}$$

Clearly, Eq. (6) agrees with Eq. (40) if T_H coincides with T_{eff}. From Eqs. (5) and (20), one obtains

$$T_H = T_m - \Delta T\;\exp\left(-\sigma\sqrt{\frac{\Omega}{2}}\right)\;\left[-\cos\left(\sigma\sqrt{\frac{\Omega}{2}}\right)\;\sin(\omega\,t)\right.$$
$$\left.+\sin\left(\sigma\sqrt{\frac{\Omega}{2}}\right)\cos(\omega\,t)\right] \quad . \tag{42}$$

Equations (41) and (42) show that T_H coincides with T_{eff} if

$$A = -\cos\left(\sigma\sqrt{\frac{\Omega}{2}}\right)\;\exp\left(-\sigma\sqrt{\frac{\Omega}{2}}\right) \quad , \tag{43}$$

$$B = \sin\left(\sigma\sqrt{\frac{\Omega}{2}}\right)\exp\left(-\sigma\sqrt{\frac{\Omega}{2}}\right) \quad . \tag{44}$$

A comparison between the values of A and B obtained numerically in this paper and the approximate values given by Eqs. (43) and (44) is illustrated in Figures 7 and 8, where A and B are plotted versus the logarithm base 10 of Ω, for $\sigma = 2$, in the range $0.0003 \leq \Omega \leq 0.3$. The figures show that a strong disagreement between the correct and the approximate values of A and B occurs, for high values of Ω. Therefore, the naive method employed in industrial design may yield a too rough approximation, except for very low values of Ω.

A check has been made on the steady–periodic numerical solution, namely a comparison with the fully transient numerical solution of Eqs.(7)–(10). The latter numerical solution has been also performed by Comsol Multiphysics by means of the `Time Dependent` solver. The initial condition considered is a uniform temperature distribution in the soil with value T_m. The solution has been obtained in the dimensionless domain by using the

values $\Omega = 3 \times 10^{-4}$, $\Xi = 0.18$, $\sigma = 1.5$. In Figure 9, $\dot{Q}/[k\,(T_a - T_m)]$ versus ωt is plotted in this case either using Eqs. (29) and (30) (solid line) or using the fully transient solution (dots). Figure 9 shows that the numerical solutions are in perfect agreement. In fact, the effect of the initial condition decays very rapidly and becomes negligible when $\omega t > 100$.

4 Conclusions

The steady–periodic heat transfer between buried offshore pipelines and their environment has been studied. The unsteady two dimensional conduction problem has been transformed into a steady two dimensional problem and solved numerically by means of the finite–element software package COMSOL Multiphysics (© Comsol Inc.). The results, reported through tables containing the values of two dimensionless parameters, can be employed for a wide range of values of the burying depth and of the radius of the pipeline, as well as of the thermal properties of the soil. The results obtained have been compared with those predicted by an approximate method employed in industrial design. The comparison revealed that the approximate method may be unreliable in some design conditions corresponding to a large diameter of the pipeline and to a low thermal diffusivity of the soil.

References

[1] A. Terenzi, F. Terra, External heat transfer coefficient of a partially sunken sealine, International Communications in Heat and Mass Transfer 28 (2001) 171–179.

[2] D. Hatziavramidis, H.-C. Ku, Pseudospectral solutions of laminar heat transfer problems in pipelines, Journal of Computational Physics 52 (1983) 414–424.

[3] A. Chervinsky, Y. Manheimer-Timnata, Transfer of liquefied natural gas in long insulated pipelines, Criogenics 9 (1969) 180–185.

[4] S. D. Probert, C. Y. Chu, Laminar flows of heavy-fuel oils through internally insulated pipelines, Applied Energy 15 (1983) 81–98.

[5] V. J. Lunardini, Heat Transfer in Cold Climates, Van Nostrand Reinhold Co, New York, 1981.

[6] A. N. Tichonov, A. A. Samarskij, Equazioni della Fisica Matematica, Mir, Mosca, 1981.

[7] H. S. Carslaw, J. C. Jaeger, Conduction of heat in solids, Oxford University Press, Glasgow, 1947, Chapter III.

Appendix

Let us consider an isothermal horizontal plane, kept at the constant temperature T_a, which is buried at a depth H from the ground surface, whose temperature varies in time according to Eq.(3) (see Figure 10).

In steady–periodic regime, the temperature distribution in the soil is given by [7]

$$T(X,t) = T_m + \frac{T_a - T_m}{H}\, X + \Delta T\, C\, \sin(\omega t + \phi) \quad , \tag{A1}$$

$$C = \left[\frac{\cosh(2\beta) - \cos(2\beta)}{\cosh(2\gamma) - \cos(2\gamma)}\right]^{\frac{1}{2}} \quad , \tag{A2}$$

$$\phi = \arctan\left(\frac{\cosh\beta\, \sinh\gamma\, \sin\beta\, \cos\gamma - \sinh\beta\, \cosh\gamma\, \cos\beta\, \sin\gamma}{\sinh\beta\, \sinh\gamma\, \cos\beta\, \cos\gamma + \cosh\beta\, \cosh\gamma\, \sin\beta\, \sin\gamma}\right) \quad , \tag{A3}$$

$$\beta = \sqrt{\frac{\omega}{2\alpha}}\,(H - X) \quad , \quad \gamma = \sqrt{\frac{\omega}{2\alpha}}\, H \quad . \tag{A4}$$

The thermal power per unit area which flows from the isothermal surface to the ground can be evaluated as

$$q = k\, \left.\frac{\partial T}{\partial X}\right|_{X=H} \quad . \tag{A5}$$

According to the approximate method, the thermal power exchanged per unit area is

$$q = \frac{k}{H}\,(T_a - T_H) \quad , \tag{A6}$$

where T_H is given by Eq.(5).

Let us assume $T_a = 50\,^{\circ}\mathrm{C}$, $T_m = 19.5\,^{\circ}\mathrm{C}$, $\Delta T = 5.5\,^{\circ}\mathrm{C}$ and consider a soil with the following thermal properties: $k = 2\ \mathrm{W/(m\,K)}$, $\alpha = 5 \cdot 10^{-7}\ \mathrm{m^2/s}$. A comparison of the thermal power per unit area given by Eq.(A5) and that given by Eq.(A6) is illustrated in Figure 11 for $H = 1\,\mathrm{m}$ and in Figure 12 for $H = 6\,\mathrm{m}$. In both Figures, the thin line refers to Eq.(A6) (approximate method), while the thick line refers to the analytical solution, given by Eq.(A5). The Figures show that while for $H = 1\,\mathrm{m}$ the results of the approximate method can be considered as acceptable, for $H = 6\,\mathrm{m}$ the approximate method underestimates the amplitude of the fluctuations of the thermal power and predicts a wrong phase of these oscillations.

Figure captions

Figure 1 – *Computational domain and boundary conditions.*

Figure 2 – *Dimensionless computational domain and boundary conditions.*

Figure 3 – *The unstructured grid adopted together with a magnification of the refinement made near the pipeline*

Figure 4 – *Amplitude of the dimensionless temperature oscillations for* $\sigma = 10$ *and* $\Omega = 0.3$.

Figure 5 – *Amplitude of the dimensionless temperature oscillations for* $\sigma = 1.2$ *and* $\Omega = 0.0003$.

Figure 6 – *Phase of the dimensionless temperature oscillations for* $\sigma = 1.2$ *and* $\Omega = 0.0003$.

Figure 7 – *Plots of A versus* $\log_{10}\Omega$ *for* $\sigma = 2$*, according to Eq.(29) (thick line) and to Eq. (44) (thin line).*

Figure 8 – *Plots of B versus* $\log_{10}\Omega$ *for* $\sigma = 2$*, according to Eq.(29) (thick line) and to Eq. (44) (thin line).*

Figure 9 – *Values of* $\dot{Q}/[k\,(T_a - T_m)]$ *versus* ωt*. Comparison between the steady–periodic numerical solution and the fully transient numerical solution.*

Figure 10 – *Isothermal horizontal plane buried at a depth* H*. The temperature of the ground surface in* $X = 0$ *varies according to Eq.(3).*

Figure 11 – *Plots of the thermal power* q *exchanged per unit area versus time* t*, for* $H = 1\text{m}$*, according to the analytical solution given by Eq.(A5) (thick line) and to the approximate method given by Eq.(A6) (thin line).*

Figure 12 – *Plots of the thermal power* q *exchanged per unit area versus time* t*, for* $H = 6\text{m}$*, according to the analytical solution given by Eq.(A5) (thick line) and to the approximate method given by Eq.(A6) (thin line).*

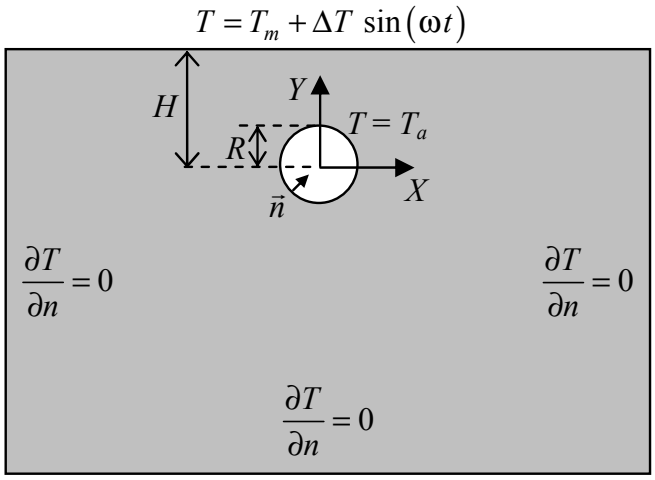

Figure 1

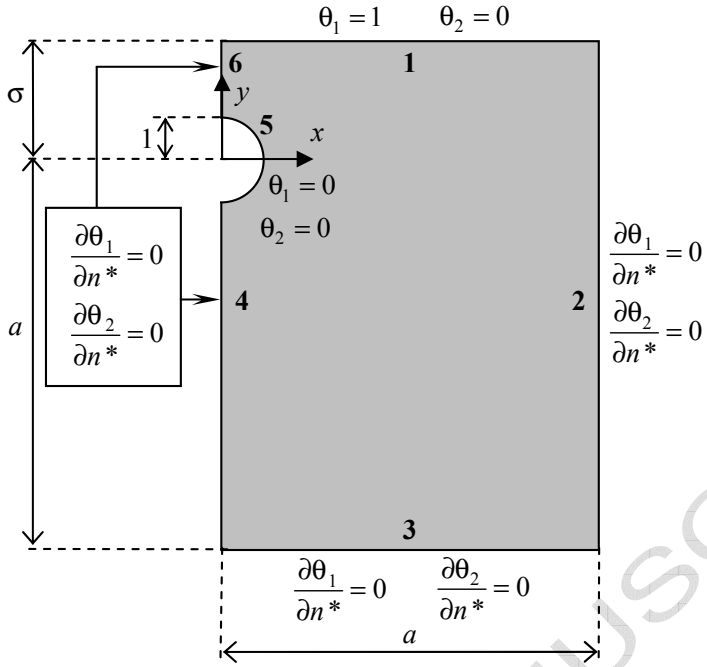

Figure 2

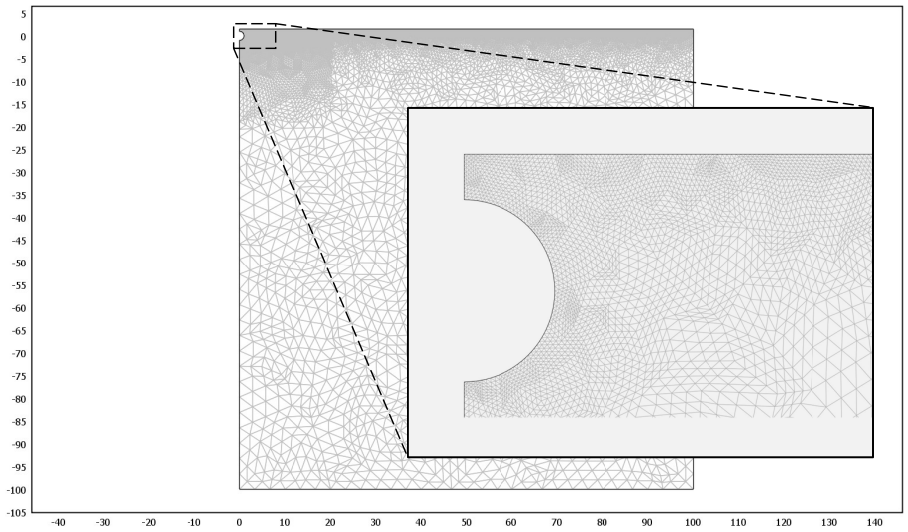

Figure 3

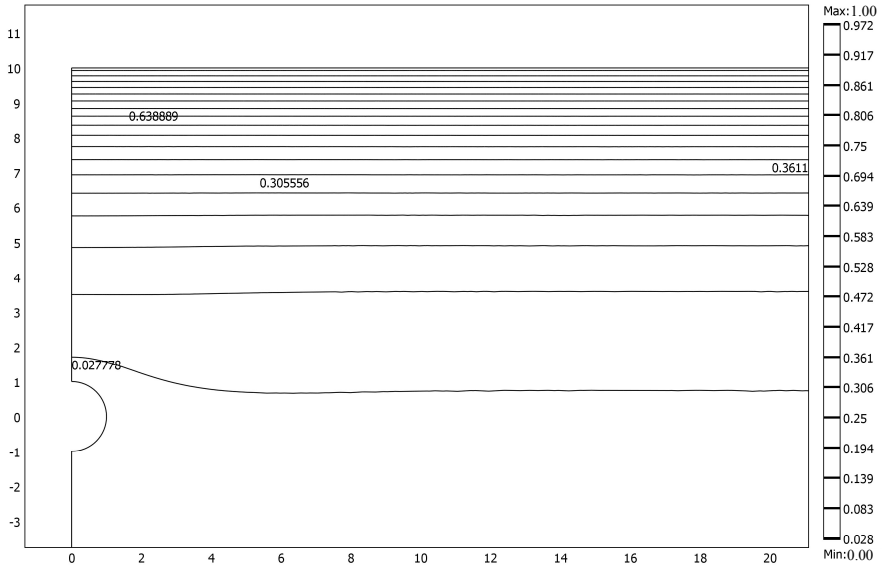

Figure 4

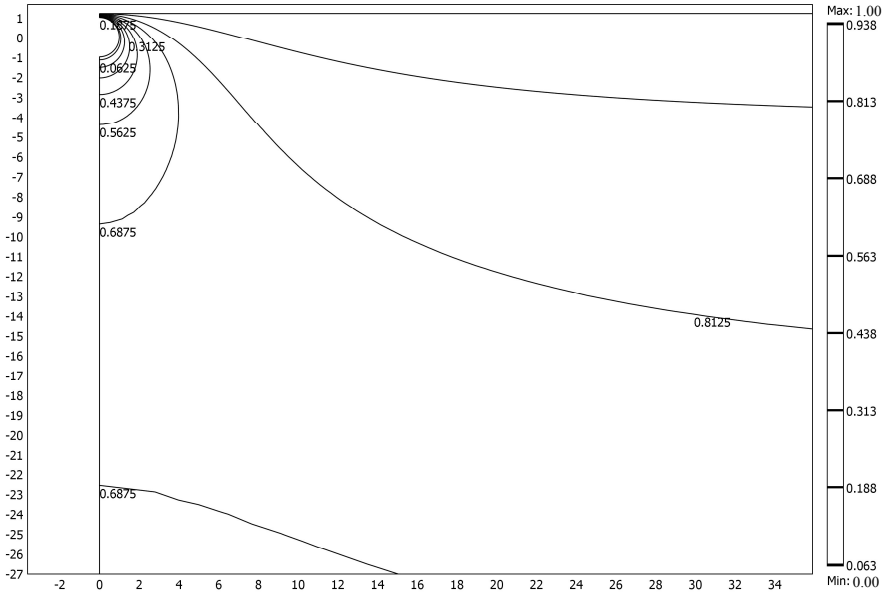

Figure 5

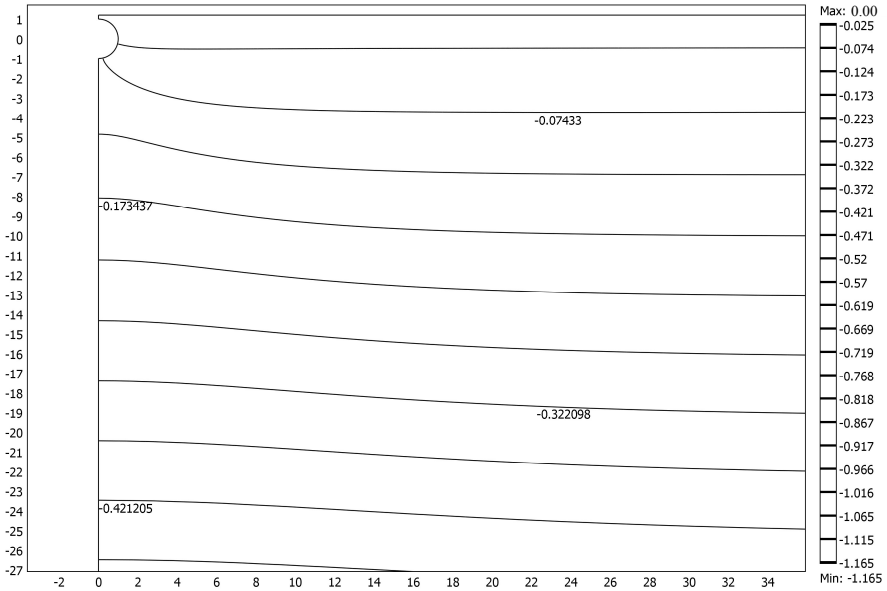

Figure 6

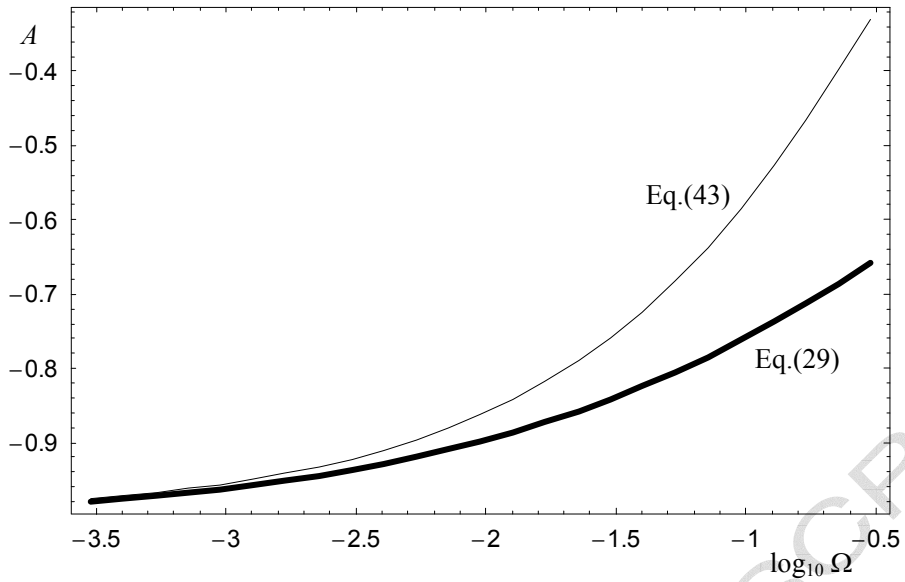

Figure 7

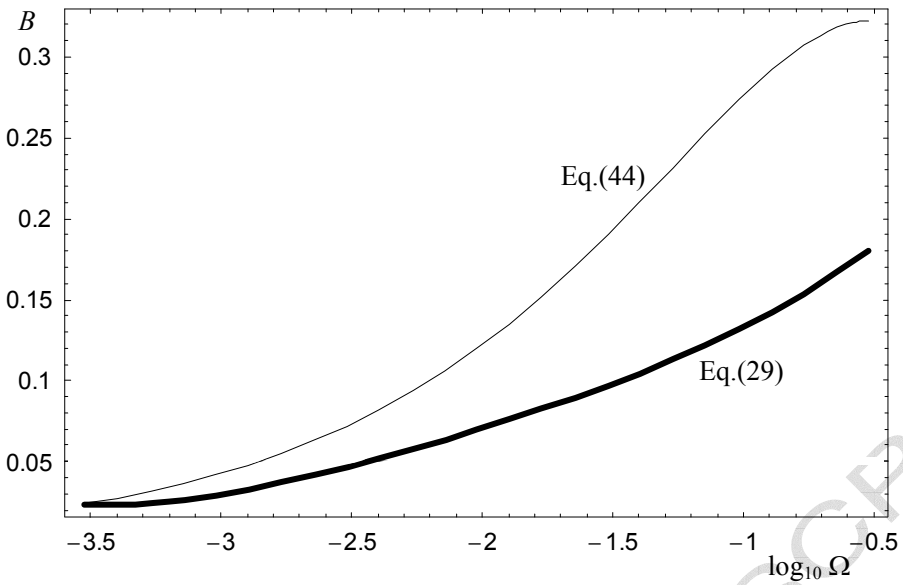

Figure 8

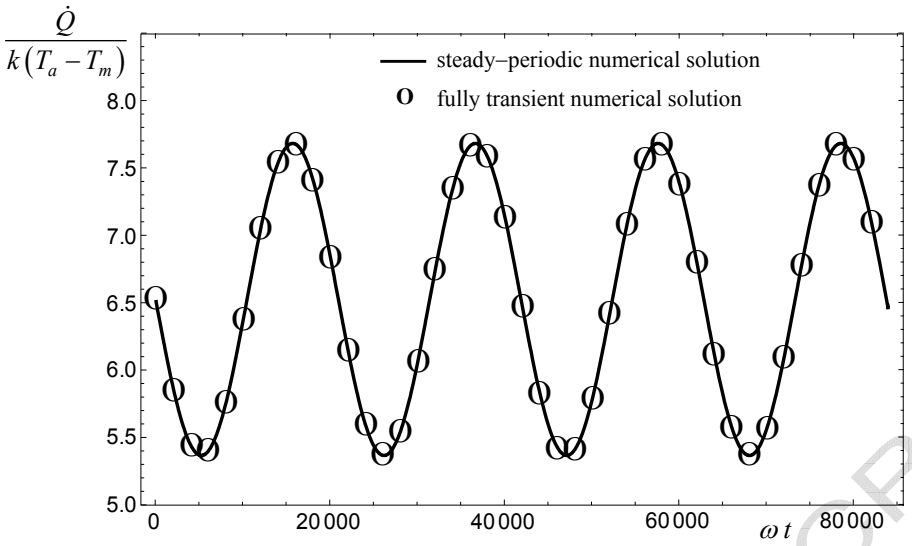

Figure 9

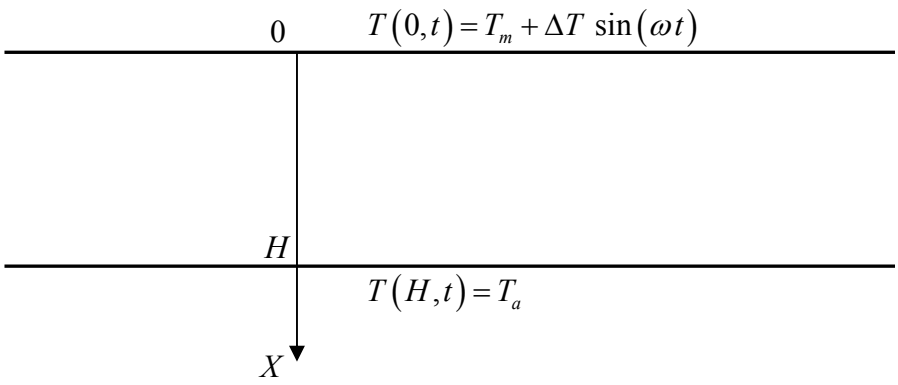

Figure 10

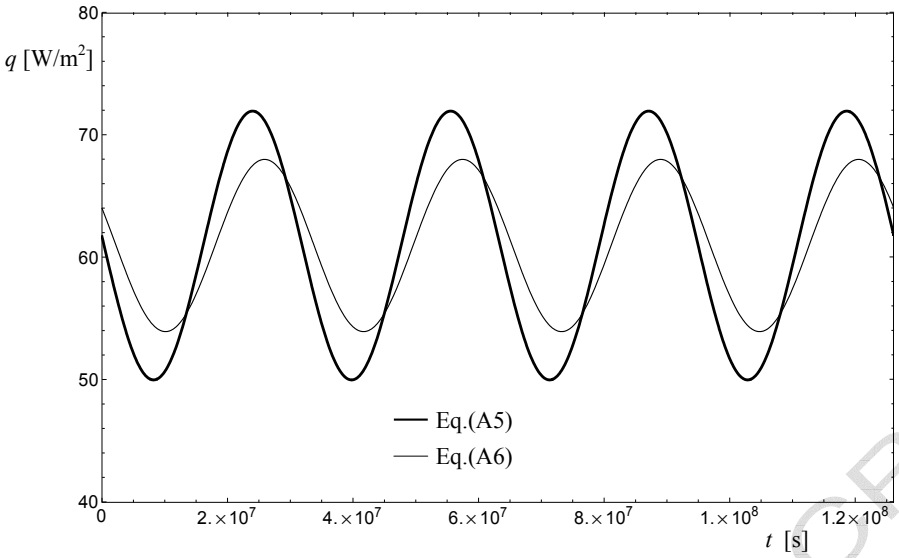

Figure 11

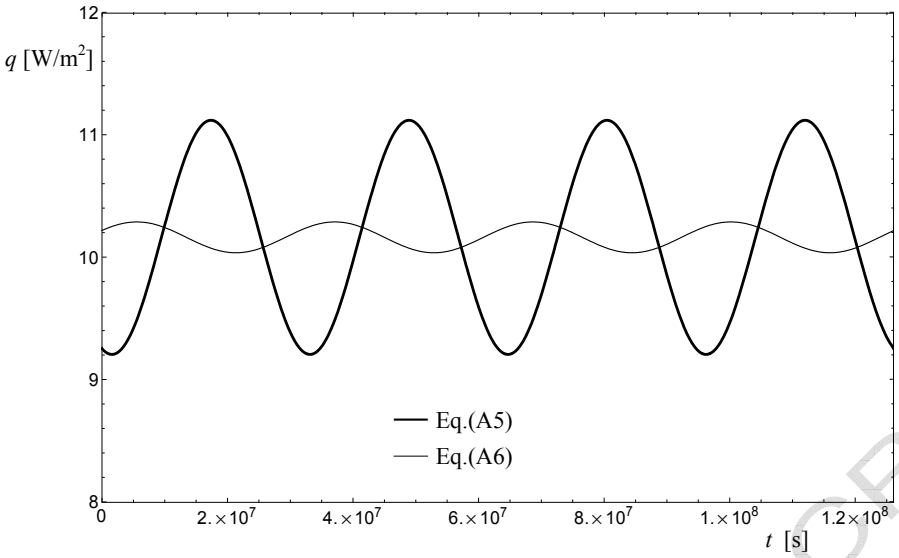

Figure 12

Table 1: Values of A and B for $\sigma = 1.2$ and $\sigma = 1.5$.

	$\sigma = 1.2$		$\sigma = 1.5$	
Ω	A	B	A	B
0.0003	-0.9920	0.009141	-0.9863	0.01526
0.001	-0.9855	0.01186	-0.9754	0.01971
0.01	-0.9592	0.02889	-0.9321	0.04738
0.05	-0.9224	0.04590	-0.8722	0.07501
0.1	-0.9010	0.05424	-0.8376	0.08915
0.2	-0.8762	0.06358	-0.7973	0.1058
0.3	-0.8599	0.06984	-0.7707	0.1175

Table 2: Values of A and B for $\sigma = 2$ and $\sigma = 4$.

	$\sigma = 2$		$\sigma = 4$	
Ω	A	B	A	B
0.0003	-0.9789	0.02329	-0.9530	0.04930
0.001	-0.9623	0.02986	-0.9182	0.06188
0.01	-0.8970	0.07042	-0.7857	0.1382
0.05	-0.8090	0.1112	-0.6145	0.2174
0.1	-0.7584	0.1333	-0.5098	0.2616
0.2	-0.6986	0.1607	-0.3728	0.3056
0.3	-0.6580	0.1803	-0.2730	0.3214

Table 3: Values of A and B for $\sigma = 6$ and $\sigma = 10$.

	$\sigma = 6$		$\sigma = 10$	
Ω	A	B	A	B
0.0003	-0.9287	0.07171	-0.8816	0.1105
0.001	-0.8784	0.08875	-0.8050	0.1345
0.01	-0.6906	0.1908	-0.5193	0.2696
0.05	-0.4435	0.2895	-0.1389	0.3095
0.1	-0.2833	0.3210	0.03150	0.2136
0.2	-0.09150	0.2974	0.08847	0.06089
0.3	0.01094	0.2381	0.06136	-0.001761